nature biotechnology

Multiplexed electrical detection of cancer markers with nanowire sensor arrays

Gengfeng Zheng[1,4], Fernando Patolsky[1,4], Yi Cui[1], Wayne U Wang[1,2] & Charles M Lieber[1,3]

We describe highly sensitive, label-free, multiplexed electrical detection of cancer markers using silicon-nanowire field-effect devices in which distinct nanowires and surface receptors are incorporated into arrays. Protein markers were routinely detected at femtomolar concentrations with high selectivity, and simultaneous incorporation of control nanowires enabled discrimination against false positives. Nanowire arrays allowed highly selective and sensitive multiplexed detection of prostate specific antigen (PSA), PSA-α1-antichymotrypsin, carcinoembryonic antigen and mucin-1, including detection to at least 0.9 pg/ml in undiluted serum samples. In addition, nucleic acid receptors enabled real-time assays of the binding, activity and small-molecule inhibition of telomerase using unamplified extracts from as few as ten tumor cells. The capability for multiplexed real-time monitoring of protein markers and telomerase activity with high sensitivity and selectivity in clinically relevant samples opens up substantial possibilities for diagnosis and treatment of cancer and other complex diseases.

Genomics and proteomics research has elucidated many new biomarkers that have the potential to greatly improve disease diagnosis[1–3]. The availability of multiple biomarkers is believed to be especially important in the diagnosis of complex diseases like cancer[4,5], for which disease heterogeneity makes tests of single markers, such as prostate specific antigen (PSA), inadequate. Patterns of multiple cancer markers might, however, provide the information necessary for robust diagnosis of disease in any person within a population[6,7]. Moreover, detection of markers associated with different stages of disease pathogenesis could further facilitate early detection.

Widespread use of cancer markers in healthcare will ultimately depend upon the development of techniques that allow rapid, multiplexed detection of many markers with high selectivity and sensitivity. This goal has not been attained with any existing method, including the enzyme-linked immunosorbent assay (ELISA)[8], a common clinical approach for protein marker detection, surface plasmon resonance (SPR)[9,10], nanoparticles[11–14], microcantilevers[15] and carbon nanotubes[16,17].

Here we present label-free, real-time multiplexed detection of protein cancer markers with high selectivity and femtomolar sensitivity using antibody-functionalized, silicon-nanowire field-effect sensors. Previously, silicon-nanowire[18] and carbon-nanotube[16] devices have been used to detect binding and unbinding of proteins in aqueous solutions. However, this previous work did not demonstrate high sensitivity, nor did it show a capability for selective multiplexed detection of different proteins[19]. To overcome previous limitations, we have developed integrated nanowire arrays in which distinct nanowires and surface receptors can be incorporated as individual device elements. We characterized the sensitivity and selectivity limits of these devices and demonstrated simultaneous quantitative detection of multiple protein markers at femtomolar concentrations, including measurements in undiluted serum samples. In addition, we carried out direct measurements of the binding, activity and small-molecule inhibition of telomerase from unamplified extracts of as few as ten tumor cells using nucleic acid–modified nanowire devices.

RESULTS

Array design and characteristics

The conversion of silicon-nanowire field-effect transistors into sensors for cancer protein marker detection was carried out by attaching monoclonal antibodies (mAbs) to the nanowire surfaces after device fabrication. The basic linkage chemistry is similar to that used previously for protein microarrays[20,21] and silicon-nanowire sensors for viruses and small molecules[22,23], and involves three key steps. First, aldehyde propyltrimethoxysilane (APTMS) is coupled to oxygen plasma–cleaned silicon-nanowire surfaces to present terminal aldehyde groups at the nanowire surface. Second, the aldehyde groups are coupled to mAbs. Third, unreacted free aldehyde groups are blocked by reaction with ethanolamine. In these studies, we show how this surface chemistry affects the nanowire device sensitivity and selectivity, which are critical for development of a viable multiplexed detection technology.

The basic nanowire sensor chip (**Fig. 1a**; see **Supplementary Fig. 1** online) consists of integrated, electrically addressable silicon nanowires with the potential for ~200 individually addressable devices. Our basic array design enables incorporation of different types of addressable nanowires, for example, p-type and n-type doped silicon nanowires, during fabrication steps to form the addressable electrical contacts; that is, solutions of the different nanowires can be sequentially assembled in different regions of the device, and then

[1]Department of Chemistry and Chemical Biology, [2]Biophysics Program and [3]Division of Engineering and Applied Science, 12 Oxford Street, Harvard University, Cambridge, Massachusetts 02138, USA. [4]These authors contributed equally to the work. Correspondence should be addressed to C.M.L. (cml@cmliris.harvard.edu).

Received 4 April; accepted 26 July; published online 18 September 2005; doi:10.1038/nbt1138

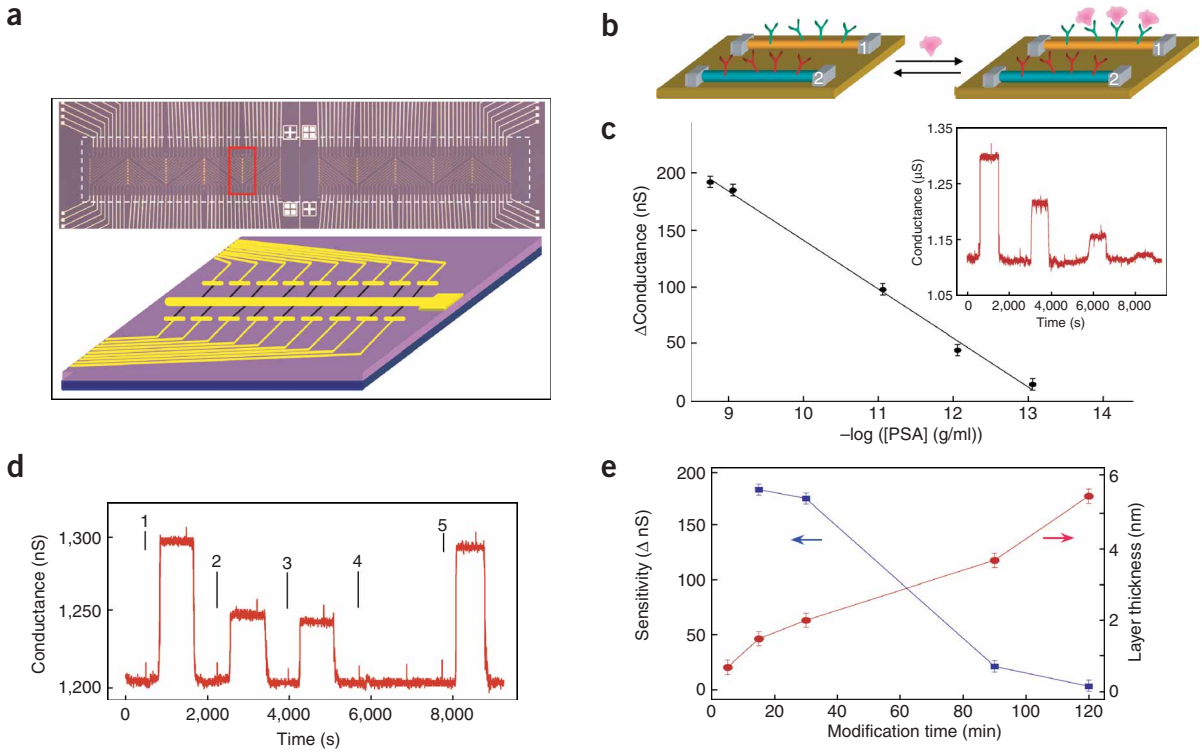

Figure 1 Nanowire sensor arrays and detector properties. (**a**) Optical image (top) of a nanowire device array. The white lines correspond to the silicon nitride passivated metal electrodes that connect to individual nanowire devices. The red rectangle highlights one of the repeated (vertical) regions where the nanowire devices are formed (see **Supplementary Fig. 1** online for high resolution images of devices). The position of the microfluidic channel used to deliver sample is highlighted by the dashed white rectangle and has a total size of 6 mm × 500 μm, length × width. The image field is 8 mm × 1.2 mm. The schematic (bottom) shows details of metal electrodes (golden lines) connecting nanowires (blue lines) in this region with orientation rotated 90° relative to red rectangle. (**b**) Schematic showing two nanowire devices, 1 and 2, within an array, where the nanowires are modified with different (1, green; 2, red) antibody receptors. A cancer marker protein that binds specifically to its receptor (on nanowire-1) will produce a conductance change characteristic of the surface charge of the protein only on nanowire-1. (**c**) Change in conductance versus concentration of PSA for a p-type silicon nanowire modified with PSA-Ab1 receptor. Inset: Conductance-versus-time data recorded after alternate delivery of PSA and pure buffer solutions; the PSA concentrations were 0.9 ng/ml, 9 pg/ml, 0.9 pg/ml and 90 fg/ml, respectively. The buffer solutions used in all measurements were 1 μM phosphate (potassium salt) containing 2 μM KCl, pH = 7.4. (**d**) Conductance-versus-time data recorded for a PSA-Ab1-modified p-type silicon nanowire after alternate delivery of the following protein and pure buffer solutions: (1) 9 pg/ml PSA, (2) 0.9 pg/ml PSA, (3) 0.9 pg/ml PSA and 10 μg/ml BSA, (4) 10 μg/ml BSA and (5) 9 pg/ml PSA. (**e**) Thickness dependence (red curve) of aldehyde silane layer on the SiNW surfaces extracted from AFM measurements after different modification time of the aldehyde propyltrimethoxysilane, and sensitivity dependence (blue curve) of detection of 1 ng/ml of PSA, after different modification time using a p-type SiNW device.

electrical contacts are formed in parallel by photolithography and metal deposition steps. In addition, different receptors can be printed on the nanowire device array to allow selective multiplexed detection (**Fig. 1b**). Selective binding of cancer marker proteins to surface-linked mAbs should produce a conductance change in the corresponding receptor-modified silicon-nanowire device but not in devices lacking the specific antibody receptor. In the case of a p-type (boron-doped) silicon nanowire, applying a positive gate voltage depletes carriers and reduces the conductance, whereas applying a negative gate voltage leads to an accumulation of carriers and an increase in conductance (the opposite effect occurs in n-type semiconductors). The dependence of the conductance on gate voltage makes field-effect transistors natural candidates for electrically based sensing since the electric field resulting from binding of a charged species to the gate dielectric is analogous to applying a voltage using a gate electrode. Thus, the conductance of a p-silicon nanowire will increase (decrease) when a protein with negative (positive) surface charge binds to the antibody receptor, whereas the opposite response should be observed for an n-type (phosphorus-doped) silicon nanowire[18].

The sensitivity limits of our silicon-nanowire devices were first determined by measuring conductance changes as the solution concentration of PSA was varied, using devices modified with mAbs for PSA (Ab1). Representative time-dependent data (inset, **Fig. 1c**) show a well-defined conductance increase and subsequent return to baseline when PSA solution and pure buffer, respectively, are alternately delivered through a microfluidic channel to the devices. A plot of these data (**Fig. 1c**) shows that the conductance change is directly proportional to the solution PSA concentration for values from ~5 ng/ml down to 90 fg/ml.

There are several key features of these data. First, the reversibility of the conductance changes demonstrates that nonspecific, irreversible protein binding does not occur to a measurable extent on the devices. Second, the increases in conductance with PSA binding to the Ab1-linked, p-type nanowire devices are consistent with binding of a protein with negative overall charge, as expected from the pI of PSA, 6.8 (ref. 24), and the pH, 7.4, of our experiments. Third, these data show that direct, label-free detection of PSA is routinely achieved with a signal-to-noise ratio >3 for concentrations down to 75 fg/ml

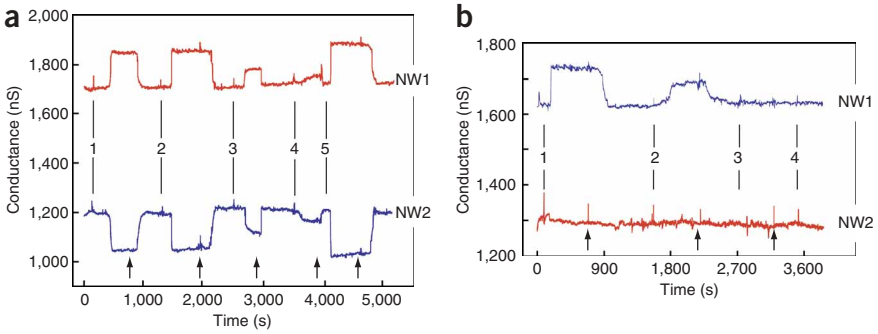

Figure 2 Multiplexed detection with nanowire arrays. (**a**) Complementary sensing of PSA using p-type (NW1) and n-type (NW2) silicon-nanowire devices in the same array. The vertical solid lines correspond to times at which PSA solutions of (1) 0.9 ng/ml, (2) 0.9 ng/ml, (3) 9 pg/ml, (4) 0.9 pg/ml and (5) 5 ng/ml were connected to the microfluidic channel. (**b**) Conductance-versus-time data recorded simultaneously from two p-type silicon-nanowire devices in an array, where NW1 was functionalized with PSA Ab1, and NW2 was modified with ethanolamine. The vertical lines correspond to times when solutions of (1) 9 pg/ml PSA, (2) 1 pg/ml PSA, (3) 10 μg/ml BSA, (4) a mixture of 1 ng/ml PSA and 10 μg/ml PSA Ab1 were connected to the microfluidic channel. Black arrows in **a** and **b** correspond to the points where the solution flow was switched from protein to pure buffer solutions.

or ~2 fM. Similar ultrasensitive detection was achieved in studies of carcinoembryonic antigen (CEA), 100 fg/ml or 0.55 fM, and mucin-1, 75 fg/ml or 0.49 fM, (see **Supplementary Fig. 2** online) using silicon-nanowire devices modified with mAbs for CEA and mucin-1, respectively.

We further investigated the devices' reproducibility and selectivity in competitive binding experiments with bovine serum albumin (BSA) (**Fig. 1d**). Conductance-versus-time measurements recorded on a silicon-nanowire device modified with Ab1 showed similar conductance changes as above when 9 and 0.9 pg/ml solutions of PSA were delivered to the device. These results show that reproducible device-to-device sensitivity was achieved. Moreover, delivery of a solution containing 0.9 pg/ml PSA and 10 μg/ml BSA showed the same conductance increase as a solution containing only PSA at this concentration, whereas no conductance change was observed when the BSA solution alone was delivered. These latter data demonstrate excellent selectivity and also show that high sensitivity was not lost even with a 10-million-fold higher concentration of other proteins in solution.

We investigated the devices' modification chemistry to define their sensitivity limits. Atomic force microscopy measurements of the initial aldehyde-silane layer thickness on single nanowires (**Fig. 1e**) showed a systematic increase with modification time. This thickness increase is consistent with previous studies showing that similar silane reagents can form multilayers[25,26]. Measurements of sensitivity showed that the sensor response decreases rapidly for initial reaction times >30 min. The observed decrease in sensitivity is consistent with expectations for a field-effect sensing device[27], and moreover, shows that the surface modification chemistry must be controlled to achieve reproducible high-sensitivity devices.

Multiplexed detection with nanowire arrays

For our initial studies of multiplexed detection, we used an array containing both p-type and n-type silicon-nanowire devices modified with Ab1. The incorporation of p- and n-type nanowires in a single sensor chip enables discrimination of possible electrical cross-talk and/or false-positive signals by correlating the response versus time from the two types of device elements. Notably, simultaneous conductance-versus-time data recorded from p-type nanowire (NW1, **Fig. 2a**) and n-type nanowire (NW2, **Fig. 2a**) devices after introduction of 0.9 ng/ml of PSA showed a conductance increase in NW1 and a conductance decrease in NW2, whereas the conductance returned to the baseline value of each device after introduction of buffer solution without PSA. The magnitudes of the conductance changes in the two devices were nearly the same and consistent with the concentration-dependent conductance measurements (**Fig. 1**). Similar behavior was observed with different concentrations of PSA (**Fig. 2a**); that is, the p- and n-type devices showed concentration-dependent increases and decreases, respectively, in conductance when the solution was alternated between PSA and buffer.

These experiments demonstrate key points about multiplexed electrical detection with nanowire devices. First, the complementary conductance changes observed for the p-type and n-type elements are consistent with specific binding of PSA to field-effect devices, since the negatively charged protein will cause accumulation and depletion of charge carriers in the p-type and n-type nanowire elements, respectively. Second, the complementary electrical signals from p- and n-type devices provide a simple yet robust means for detecting false-positive signals from either electrical noise or nonspecific binding of protein to one device; that is, real and selective binding events must show complementary responses in the p- and n-type devices. The presence of correlated conductance signals in both devices (**Fig. 2a**), which occur at points when buffer and PSA/buffer solutions are changed, illustrates clearly how this multiplexing capability can be used to distinguish unambiguously noise from protein-binding signals.

Table 1 Summary of multiplexed detection experiments using nanowire devices modified with mAb receptors specific for free PSA (f-PSA), Ab1 and cross-reactive for f-PSA and PSA-ACT complex, Ab2

		Conductance change, nS	
Protein sample	[Protein] pg/ml	NW1-Ab1	NW2-Ab2
f-PSA	1,700	192	154
f-PSA	850	185	132
f-PSA	8.5	98	81
f-PSA	0.85	45	50
f-PSA	0.085	15	10
PSA-ACT	3,200	ND	143
PSA-ACT	320	ND	124
PSA-ACT	3.2	ND	67
PSA-ACT	0.32	ND	19
f-PSA, PSA-ACT, Ab1	850, 3,200, 1×10^7	ND	140
f-PSA, PSA-ACT, Ab1	8.5, 320, 1×10^7	ND	118
f-PSA, PSA-ACT, Ab1	0.85, 3,200, 1×10^7	ND	138
f-PSA, PSA-ACT, Ab1	850, 0.32, 1×10^7	ND	15
f-PSA, Ab1	850, 1×10^7	ND	ND

ND corresponds to no detected conductance change. Sensor data used to obtain conductance changes are shown in **Supplementary Figure 3** online.

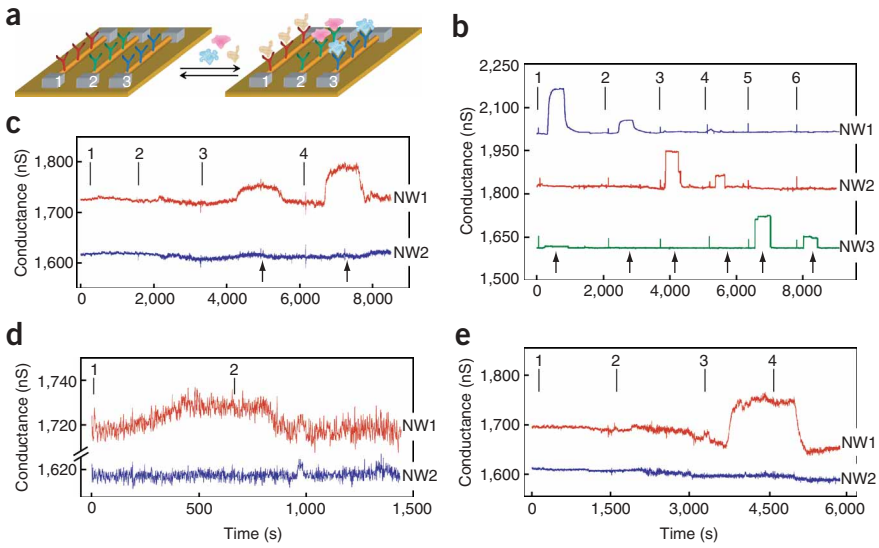

Figure 3 Multiplexed detection of cancer marker proteins. (**a**) Schematic illustrating multiplexed protein detection by three silicon-nanowire devices in an array. Devices 1, 2 and 3 are fabricated from similar nanowires, and then differentiated with distinct mAb receptors (1, red; 2, green; 3, blue) specific to three different cancer markers. (**b**) Conductance-versus-time data recorded for the simultaneous detection of PSA, CEA and mucin-1 on p-type silicon-nanowire array in which NW1, NW2 and NW3 were functionalized with mAbs for PSA, CEA and mucin-1, respectively. The solutions were delivered to the nanowire array sequentially as follows: (1) 0.9 ng/ml PSA, (2) 1.4 pg/ml PSA, (3) 0.2 ng/ml CEA, (4) 2 pg/ml CEA, (5) 0.5 ng/ml mucin-1, (6) 5 pg/ml mucin-1. Buffer solutions were injected following each protein solution at points indicated by black arrows. (**c**) Conductance-versus-time data recorded for the detection of PSA-containing donkey serum samples on a p-type silicon-nanowire array in which NW1 was functionalized with Ab1 and NW2 was passivated with ethanolamine. The solutions were delivered to the nanowire array sequentially as follows: (1) 1 μM phosphate buffer + 2 μM KCl, pH = 7.4, (2) donkey serum, (3) a mixture of donkey serum and 90 pg/ml of PSA, (4) a mixture of donkey serum and 0.9 ng/ml of PSA. The donkey serum was injected at points indicated by the black arrows. (**d**) Conductance-versus-time data recorded for the same two p-type silicon-nanowire devices after addition of (1) a mixture of donkey serum and 0.9 pg/ml of PSA, (2) donkey serum. (**e**) Conductance-versus-time data recorded for the detection of PSA-containing human serum samples on a p-type silicon-nanowire array in which NW1 was functionalized with Ab1 and NW2 was passivated with ethanolamine. The solutions were delivered to the nanowire array sequentially as follows: (1) 1 μM phosphate buffer + 2 μM KCl, pH = 7.4, (2) a mixture of human serum preblocked with 10 μg/ml Ab1, (3) human serum and (4) same as (2).

We carried out a second test of multiplexing capabilities using a device array consisting of p-type silicon-nanowire elements with either PSA Ab1 receptors (NW1, **Fig. 2b**) or surfaces passivated with ethanolamine (NW2, **Fig. 2b**). Simultaneous measurements of the conductance of NW1 and NW2 show that well-defined, concentration-dependent conductance increases were only observed in NW1 upon delivery of PSA solutions (9 and 1 pg/ml), although small conductance spikes were observed in both devices at the points where PSA and buffer solutions were changed. Delivery of BSA at 10 μg/ml showed no response in either NW1 or NW2, and subsequent delivery of a solution of PSA (1 ng/ml) and Ab1 (10 μg/ml), which complexes the free PSA, did not cause measurable conductance changes in either device. Together, these multiplexing experiments demonstrate that the electronic signals measured can be readily attributed to selective marker-protein binding, show that our surface passivation chemistry effectively prevents nonspecific protein binding, and provide a robust means for discriminating against false-positive signals arising from either electronic noise or nonspecific binding.

Multiplexed detection of cancer markers

To test the capabilities of the nanowire arrays for multiplexed detection of marker proteins relevant to cancer, we first focused on free PSA (f-PSA) and PSA-α1-antichymotrypsin (PSA-ACT) complex, which are generally measured in the diagnosis of prostate cancer[28–30]. We fabricated a device array from p-type silicon-nanowire elements that were then modified either with mAbs for f-PSA, Ab1, or mAbs that cross-react with f-PSA and the PSA-ACT complex, Ab2. Simultaneous conductance measurements of NW1, which was modified with Ab1, and NW2, which was modified with Ab2, were carried out for a wide range of conditions (see **Supplementary Fig. 3** online) and are summarized in **Table 1**. The data show that delivery of f-PSA resulted in concentration-dependent conductance changes in both NW1 and NW2, whereas the introduction of PSA-ACT yielded concentration-dependent conductance changes only in NW2. In addition, control experiments in which solutions of f-PSA, PSA-ACT and Ab1 were delivered showed concentration-dependent conductance changes in NW2 but not NW1, because f-PSA was blocked by Ab1 present in the solution. These multiplexing results demonstrate selective, high-sensitivity detection of both markers and show that nanowire sensor arrays measured the f-PSA and PSA-ACT concentrations in a single real-time assay.

We also investigated multiplexed detection of three cancer marker proteins, f-PSA, CEA and mucin-1, using silicon-nanowire devices functionalized with mAbs for f-PSA (NW1), CEA (NW2) and mucin-1 (NW3) (**Fig. 3a**). Conductance-versus-time measurements were recorded simultaneously from NW1, NW2 and NW3 as different protein solutions were sequentially delivered (**Fig. 3b**). First, introduction of f-PSA and buffer solutions led to concentration-dependent conductance increases only when NW1 was exposed to PSA solution; no conductance changes were observed in NW2 or NW3. Similarly, introduction of CEA solutions yielded concentration-dependent conductance changes only in NW2, whereas subsequent delivery of mucin-1 solutions resulted in concentration-dependent conductance changes only in NW3. These results demonstrate multiplexed real-time, label-free marker-protein detection with sensitivity to the femtomolar level and essentially complete selectivity.

Protein detection in serum samples

Cancer diagnosis will require rapid analysis of clinically relevant samples, such as blood serum. To this end, we investigated detection of PSA in undiluted donkey and human serum samples that were desalted in a rapid and simple purification step. The measurements were made using p-type silicon-nanowire elements with either PSA Ab1 receptors (NW1, **Fig. 3c–e**) or surfaces passivated with ethanolamine (NW2, **Fig. 3c–e**) in the same sensor array.

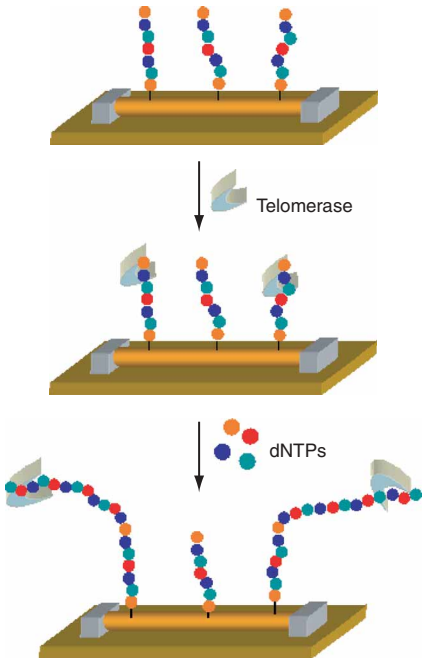

Figure 4 Schematic of the telomerase binding and activity assay. (Top) Silicon-nanowire devices modified with oligonucleotide primer. (Middle) A solution containing telomerase is delivered to the device array, and telomerase binds in a concentration-dependent process. (Bottom) Subsequent addition of dNTPs leads to telomerase-catalyzed primer extension/elongation.

Conductance-versus-time measurements recorded simultaneously from NW1 and NW2 as different donkey serum solutions were sequentially delivered to the devices are shown in **Figure 3c**,**d**. Delivery of donkey serum containing 59 mg/ml total protein did not lead to an appreciable conductance change relative to the standard assay buffer. Donkey serum solutions containing f-PSA led to concentration-dependent conductance increases only for NW1; no conductance changes were observed in NW2 (**Figs. 3c**,**d**). Well-defined conductance changes were observed for PSA concentrations as low as 0.9 pg/ml, which corresponds to a concentration ~100-billion times lower than that of the background serum proteins. Similar results were obtained for human serum samples (**Fig. 3e**). Specifically, addition of undiluted human serum, which contains f-PSA, blocked with an excess of Ab1, showed little change in baseline for either NW1 or NW2, although subsequent addition of undiluted human serum showed a well-defined conductance increase in NW1. These results clearly demonstrate the detection of cancer markers with high sensitivity and selectivity in human serum.

Telomerase detection and activity

To define further the potential of our silicon-nanowire arrays as cancer diagnostic tools, we investigated a nucleic acid–based marker assay involving detection of telomerase. Telomerase is a eukaryotic ribonucleoprotein complex[31,32] that catalyzes the addition of the telomeric repeat sequence TTAGGG to the ends of chromosomes using its intrinsic RNA as a template for reverse transcription[33,34]. Telomerase activity has been found in at least 80% of all known human cancers[35,36], but no activity was found in most of the adjacent somatic tissues, and telomerase has thus been proposed as a marker for cancer detection and as a therapeutic target.

The telomerase assay is illustrated in **Figure 4**. First, silicon-nanowire device elements within an array are functionalized with oligonucleotide primers complementary to the telomerase binding site. Second, the presence or absence of telomerase is then detected by monitoring the nanowire conductance after delivery of a sample cell extract to the device array. In the case of p-type nanowire device elements, binding should reduce the conductance, as telomerase (pI ~ 10)[37] is positively charged at physiological pH. Third, addition of deoxynucleotide triphosphates (dNTPs) leads, in the presence of telomerase, to elongation, which should produce an increase in conductance owing to the incorporation of negatively charged nucleotides near the nanowire surface.

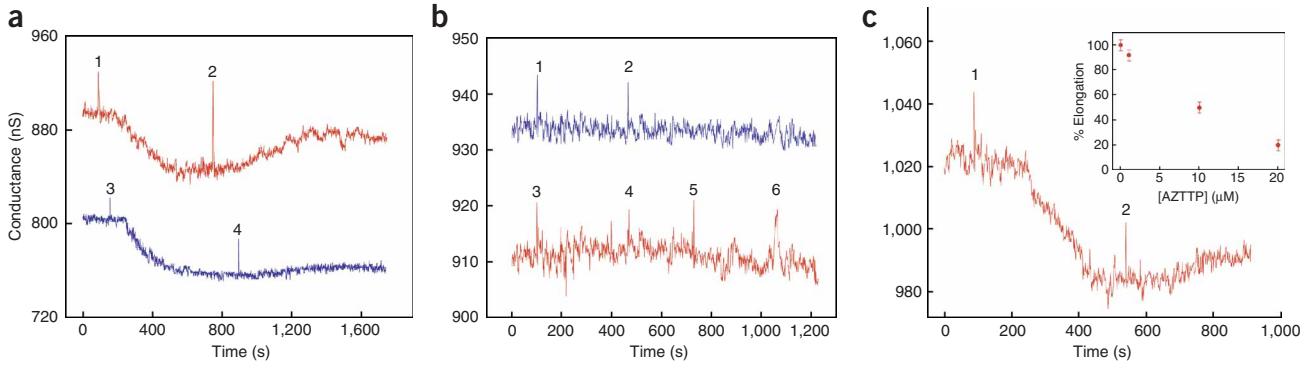

Figure 5 Detection of telomerase (**a**) Conductance-versus-time data recorded for oligonucleotide-modified p-type silicon-nanowire devices, after the introduction of (1) a solution containing extract from 100 HeLa cells and 0.4 mM dCTP, (2) a mixture all four dNTPs (dATP, dGTP, dUTP and dCTP) each at 0.1 mM, (3) a solution containing extract from 100 HeLa cells and 0.4 mM dCTP and (4) 0.4 mM dCTP only. Points (3) and (4) were recorded using a second device. (**b**) Conductance-versus-time data recorded for oligonucleotide-modified nanowire device after delivery of (1) a solution containing extract from 100,000 normal human fibroblast cells and 0.4 mM dCTP, (2) a mixture of all four dNTPs each at 0.1 mM, (3) a solution containing extract from 10,000 HeLa cells, 0.4 mM dCTP, and 5 μM oligonucleotide (sequence: 5′-TTTTTTAATCCGTCGAGCAGAGTT-3′), (4) a mixture of all four dNTPs each at 0.1 mM, (5) a solution containing extract from 10,000 heat-deactivated HeLa cells (90 °C, 10 min) and 0.4 mM dCTP and (6) a mixture of all four dNTPs each at 0.1 mM. (**c**) Conductance-versus-time data recorded on a p-type silicon-nanowire device after the introduction of (1) a solution containing extract from 100 HeLa cells and 0.4 mM dCTP, and (2) a mixture of all four dNTPs each at 0.1 mM and 20 μM AZTTP. Inset: Plot of the inhibition of elongation versus AZTTP concentration, where 100% corresponds to conductance change associated with elongation in the absence of AZTTP.

Representative conductance-versus-time data recorded from an oligonucleotide primer–modified p-type silicon-nanowire element (**Fig. 5a**) showed a well-defined conductance decrease after delivery of the extract from 100 HeLa cells. We attribute this conductance decrease to selective binding of positively charged telomerase at the surface of p-type nanowires in the array. This interpretation is unambiguously supported by the results of several additional experiments. First, the conductance decrease was directly proportional to the number of HeLa cells (and hence telomerase concentration) used to prepare the extract (see **Supplementary Fig. 4** online), as expected for an equilibrium binding process. These data also show that binding was readily detectable at the ten-cell level without amplification. Second, delivery of a solution extract prepared from 100,000 normal human fibroblasts (**Fig. 5b,** point-1) showed no conductance change. Third, delivery of HeLa cell extracts preincubated with a solution of oligonucleotide, which blocks binding to the much lower concentration of surface-bound primers, did not result in an observable conductance change (**Fig. 5b**, point-3). Finally, experiments carried out with heat-denatured HeLa cell extracts showed essentially no conductance decrease above background (**Fig. 5b**, point-5).

Telomerase activity could be monitored directly by adding dNTPs after initial telomerase binding, leading to an increase in conductance (**Fig. 5a**). This increase is consistent with the telomerase-catalyzed incorporation of negatively charged nucleotides[32,33]. In the absence of dNTPs, no significant conductance increase was observed after the telomerase binding step (**Fig. 5a**), showing that the observed increase does not correspond to unbinding of telomerase on the time scale of our experiment. In addition, the conductance increase at a fixed concentration of dNTPs was proportional to the number of HeLa cells used for the initial binding step (see **Supplementary Fig. 4** online), which shows that the overall nucleotide addition depends on the telomerase concentration bound initially to primers. These data also demonstrate that telomerase activity can be monitored at least to the ten-cell level without amplification. Further experiments showed no conductance increases when dNTPs were delivered after initial addition of (i) extract from normal human fibroblasts cells (**Fig. 5b,** point-2), (ii) HeLa cell extracts preincubated with primer-oligonucleotides (**Fig. 5b**, point-4) or (iii) heat-denatured HeLa cell extracts (**Fig. 5b**, point-6). These control experiments show clearly that conductance increases observed in the presence of dNTPs were indeed due to telomerase-catalyzed nucleotide addition[38]. Our telomerase activity measurements are distinct from current approaches based upon variations of telomeric repeat amplification protocol (TRAP)[39–43], as PCR amplification is not required to achieve high sensitivity.

Lastly, we investigated whether nanowire detectors of telomerase binding and/or activity could be used to screen for telomerase inhibitors. Delivery of a solution containing dNTPs and azido deoxythymidine triphosphate (AZTTP), a known reverse transcriptase inhibitor[44], after initial telomerase binding reduced the conductance increase associated with elongation (**Fig. 5c**). Studies of AZTTP concentration-dependent inhibition (inset, **Fig. 5c**) showed up to an 80% reduction of elongation as the AZTTP concentration was increased to 20 μM, thus demonstrating direct monitoring of telomerase inhibition.

DISCUSSION

In these studies, we have demonstrated the development and validation of nanowire sensor arrays for label-free, real-time, multiplexed electrical detection of cancer markers with ultrahigh sensitivity and excellent selectivity. The nanowire arrays were used to elucidate the surface modification details needed for ultrahigh device sensitivity, to demonstrate very good device-to-device absolute detection reproducibility and also to show two distinct approaches for simultaneous discrimination against false positives. Modification of the arrays with antibodies allowed real-time multiplexed detection of f-PSA, PSA-ACT complex, CEA and mucin-1 with good signal-to-noise ratios down to a 50- to 100-fg/ml level. Moreover, we achieved high selectivity and sensitivity to concentrations at least as low as 0.9 pg/ml in undiluted serum samples containing as much as 100-billion times more protein than the cancer marker being detected. In addition, using the same chemistry to prepare nucleic acid primer–modified devices, we showed that telomerase binding and activity could be measured down to a ten-cell level without amplification.

These results surpass previous protein detection studies with semiconductor nanowires[18] and carbon nanotubes[16,17], in which sensitivity was $\sim 10^3$ and 10^6 times lower, respectively, device-to-device reproducibility and selectivity were not addressed, and no multiplexed detection was carried out. The protein detection limits of nanowire array sensors also exceed those of most existing technologies[8–15], including ELISA sandwich assays (e.g., 3 pg/ml for PSA detection[8]). More recent work employing magnetic and gold nanoparticles[14] has attained sensitivities two orders of magnitude better than what has been achieved in our work; however, these sandwich assays require labeling and multiple chemical and biochemical manipulation steps. Label-free detection of marker proteins has also been investigated using SPR[9,10,45,46] with sensitivity limits of $\sim$10–100 pg/ml, and microcantilevers[15], with a detection limit of 0.2 ng/ml. These limits are 10^3 worse than that achieved by our nanowire arrays, and the detection times with microcantilevers are also much longer than with SPR and nanowire devices. In addition, our approach allows multiplexed detection, which will be important for improving cancer screening, diagnosis and treatment.

We believe that detection of telomerase binding and activity with nanowire sensor arrays should also facilitate cancer detection. Almost all telomerase assays used today are based upon the TRAP protocol[39–43], in which PCR is used for amplification, and fluorescence or radiolabeling is used for detection. TRAP-based assays can detect telomerase activity in as few as ten cells. Our assay achieves this same level of sensitivity but without PCR or labeling. It also facilitates studies of telomerase inhibitors.

In conclusion, we have demonstrated highly sensitive and selective multiplexed electrical detection of protein cancer markers and telomerase using arrays of silicon-nanowire field-effect devices in both ideal and clinically relevant samples of blood serum and cell extract. Simultaneous real-time measurements in the present work were limited to three distinct sensor devices, although we note that this limit was related only to available measurement electronics. At least 100 independently addressable sensor elements are available in the arrays described in this work and could be used with more sophisticated multiplexing electronics. Thus, we believe that the nanowire sensor arrays can move beyond current technologies and take advantage of information emerging from genomics and proteomics to improve the diagnosis and treatment of cancer and other complex diseases.

METHODS

Nanowire arrays fabrication. Silicon nanowires were synthesized by chemical vapor deposition using 20-nm gold nanoclusters as catalysts, silane as reactant. For p-type silicon nanowires[47], diborane was used as dopant, with a B:Si ratio of 1:4,000; for n-type silicon nanowires[48], phosphine was used as dopant, with a P:Si ratio of 1:4,000. Arrays of silicon-nanowire devices were defined

using photolithography with Ni metal contacts on silicon substrates with 600-nm-thick oxide layer. The metal contacts were passivated by subsequent deposition of ~50-nm thick Si_3N_4 coating. The spacing between source-drain electrodes (active sensor area) was 2 μm in all experiments. Protein samples were delivered to the nanowire device arrays using fluidic channels formed by a flexible poly(dimethylsiloxane) polymer channel sealed to the device chip[18], and samples were delivered through inlet/outlet connection in the polymer.

Nanowire surface modification. A two-step procedure was used to covalently link antibody receptors and oligonucleotides to the surfaces of the silicon-nanowire devices. First, the devices were reacted with a 1% ethanol solution of 3-(trimethoxysilyl)propyl aldehyde (United Chemical Technologies) for ~30 min, washed with ethanol and heated at 120 °C for 15 min. MAb receptors, anti-PSA (AbI, clone ER-PR8, NeoMarkers), anti-ACT-PSA (AbII, clone PSA1 with 59% cross-reactivity to ACT-PSA, Abcam), anti-CEA antibody (clone COL-1, Neomarkers) and anti-mucin-1 (clone B413, Abcam) were coupled to the aldehyde-terminated nanowire surfaces by reaction of 10–100 μg/ml antibody in a pH 8.4, 10 mM phosphate buffer solution containing 4 mM sodium cyanoborohydride for a period of 2–3 h. Unreacted aldehyde surface groups were subsequently passivated by reaction with ethanolamine, in the presence of 4 mM cyanoborohydride, under similar conditions for a period of 1–2 h. Device arrays for multiplexed experiments were made in the same way except that distinct antibody solutions (1% vol/vol glycerol) were spotted on different regions of the array. The antibody surface density versus reaction time was quantified by reacting Au-labeled IgG antibodies (5 nm Au-nanoparticles, Ted Pella laboratories) with aldehyde-terminated nanowires, and then imaging the modified nanowire by transmission electron microscopy.

Protein samples. PSA, PSA-ACT, CEA and mucin-1 were purchased from Calbiochem. All protein samples were used as received without further purification and diluted in the assay buffer (1 μM phosphate buffer solution containing 2 μM KCl with pH 7.4) prior to sensing measurements.

Serum samples. Donkey serum (pooled preparation obtained from normal donor herd, total protein 59 mg/ml), and human serum (from clotted human male whole blood, 40–90 mg/ml total protein) were purchased from Sigma, desalted using a microcentrifuge filter (Centricon YM-3, 3,000 MWCO, Millipore) and diluted back to the original protein concentration with the assay buffer solution (1 μM phosphate buffer, 2 μM KCl, pH 7.4) before injection into the detection system. PSA was added to donkey serum before the desalting step for data presented in the paper; however, similar results were also obtained from samples in which PSA was added after desalting.

Cell samples and nanowire modification for telomerase experiments. All cell extracts from frozen cell pellets were prepared using CHAPS lysis buffer (Centricon International, 100 μl 1× CHAPS buffer, 10 mM Tris-HCl, pH 7.5, 1 mM $MgCl_2$, 1 mM EGTA, 0.1 mM benzamidine, 0.5% CHAPS (3-[(3-cholamidopropyl)dimethylammonio] propanesulfonic acid), 5 mM α-mercaptoethanol and 10% glycerol) fractionated and stored at −80 °C until used and diluted in telomerase assay buffer (10 μM HEPES buffer, 1.5 mM KCl, 100 μM $MgCl_2$ and 10 μM EGTA, pH 7.4). Normal human fibroblast cells (ATCC), HeLa cells (Chemicon International), AZTTP (azido deoxythymidine triphosphate, Sigma-Aldrich), and dATP, dGTP, dUTP and dCTP (Sigma). Aldehyde functionalized silicon nanowires were modified with the amino-modified oligonucleotide 5′-H_2N-$(CH_2)_6$- TTTTTTAATCCGTCGAGCAGA GTT-3′ (Sigma-Genosys) in 100 mM phosphate buffer, pH 8.4, and 5 mM $NaCNBH_3$ for 2 h. The sensor array was washed using the microfluidic channel with 100 mM phosphate buffer pH 8.4, and then the telomerase assay buffer (10 μM Hepes buffer, 1.5 mM KCl, 100 μM $MgCl_2$ and 10 μM EGTA, pH 7.4).

Electrical measurements. Electrical measurements were made using lock-in detection with a modulation frequency of 79 Hz. The modulation amplitude was 30 mV and the dc source-drain potential was set at zero to avoid electrochemical reactions. Conductance-versus-time data was recorded whereas buffer solutions, or different protein solutions, were flowed through the microfluidic channel. Protein sensing experiments were performed in the microfluidic channel under a flow rate of 0.15 ml/h in 1 μM phosphate buffer solution containing 2 μM KCl with pH 7.4. Multiplexing experiments were carried out by interfacing up to three independent lock-in amplifiers to different nanowire elements within the sensor arrays; the output was recorded simultaneously as a function of time by computer through analog-to-digital converter.

We note that frequency-dependent measurements show that for a 12.6-times increase in detection frequency (from the value used in our studies) the binding time increases ~5×; that is, it takes substantially longer. This behavior suggests that electrokinetic effects, which have been reported to lead to enhancements in the local concentration of a variety of biological species[49], contribute to and enhance the observed binding kinetics in our measurements.

AFM measurements. The increase in the thickness of silicon nanowires as a function of silane modification times was measured by atomic force microscopy (AFM, Nanoscope IIIa, Digital Instruments) on a lithographically marked Au surface, to localize and measure the same nanowires each time.

Note: Supplementary information is available on the Nature Biotechnology website.

ACKNOWLEDGMENTS

We thank M. Shuman (UCSF) for helpful discussion. C.M.L. acknowledges support of this work by the Defense Advanced Research Projects Agency and the National Cancer Institute.

COMPETING INTERESTS STATEMENT

The authors declare that they have no competing financial interests.

Published online at http://www.nature.com/naturebiotechnology/
Reprints and permissions information is available online at http://npg.nature.com/reprintsandpermissions/

1. Sander, C. Genomic medicine and the future of health care. *Science* **287**, 1977–1978 (2000).
2. Etzioni, R. *et al.* The case for early detection. *Nat. Rev. Cancer* **3**, 243–252 (2003).
3. Srinivas, P.R., Kramer, B.S. & Srivastava, S. Trends in biomarker research for cancer detection. *Lancet Oncol.* **2**, 698–704 (2001).
4. Wulfkuhle, J.D., Liotta, L.A. & Petricoin, E.F. Proteomic applications for the early detection of cancer. *Nat. Rev. Cancer* **3**, 267–275 (2003).
5. Brawer, M.K. *Prostate Specific Antigen* (Marcel Dekker, New York, 2001).
6. Sidransky, D. Emerging molecular markers of cancer. *Nat. Rev. Cancer* **2**, 210–219 (2002).
7. Abeloff, M.D., Armitage, J.O., Lichter, A.S. & Niederbuber, J.E. *Clinical Oncology* (Churchill Livingstone, New York, 2000).
8. Ward, A.M., Catto, J.W.F. & Hamdy, F.C. Prostate specific antigen: biology, biochemistry and available commercial assays. *Ann. Clin. Biochem.* **38**, 633–651 (2001).
9. Campagnolo, C. *et al.* Real-Time, label-free monitoring of tumor antigen and serum antibody interactions. *J. Biochem. Biophys. Methods* **61**, 283–298 (2004).
10. Chou, S.F., Hsu, W.L., Hwang, J.M. & Chen, C.Y. Development of an immunosensor for human ferritin, a nonspecific tumor marker, based on surface plasmon resonance. *Biosens. Bioelectron.* **19**, 999–1005 (2004).
11. Alivisatos, P. The use of nanocrystals in biological detection. *Nat. Biotechnol.* **22**, 47–52 (2004).
12. Gao, X., Cui, Y., Levenson, R.M., Chung, L.W.K. & Nie, S. *In vivo* targeting and imaging with semiconductor quantum dots. *Nat. Biotechnol.* **22**, 969–976 (2004).
13. Soukka, T. *et al.* Supersensitive time-resolved immunofluorometric assay of free prostate-specific antigen with nanoparticle label technology. *Clin. Chem.* **47**, 1269–1278 (2001).
14. Nam, J.M., Thaxton, C.S. & Mirkin, C.A. Nanoparticle-based bio-bar codes for the ultrasensitive detection of proteins. *Science* **301**, 1884–1886 (2003).
15. Wu, G. *et al.* Bioassay of prostate-specific antigen (PSA) using microcantilevers. *Nat. Biotechnol.* **19**, 856–860 (2001).
16. Chen, R.J. *et al.* Noncovalent functionalization of carbon nanotubes for highly specific electronic biosensors. *Proc. Natl. Acad. Sci. USA* **100**, 4984–4989 (2003).
17. Chen, R.J. *et al.* An investigation of the mechanisms of electronic sensing of protein adsorption on carbon nanotube devices. *J. Am. Chem. Soc.* **126**, 1563–1568 (2004).
18. Cui, Y., Wei, Q.Q., Park, H.K. & Lieber, C.M. Nanowire nanosensors for highly sensitive and selective detection of biological and chemical species. *Science* **293**, 1289–1292 (2001).
19. Ferrari, M. Cancer nanotechnology: opportunities and challenges. *Nat. Rev. Cancer* **5**, 161–171 (2005).
20. MacBeath, G. & Schreiber, S.L. Printing proteins as microarrays for high-throughput function determination. *Science* **289**, 1760–1763 (2000).
21. Arenkov, P. *et al.* Protein microchips: use for immunoassay and enzymatic reactions. *Anal. Biochem.* **278**, 123–131 (2000).

22. Patolsky, F. *et al.* Electrical detection of single viruses. *Proc. Natl. Acad. Sci. USA* **101**, 14017–14022 (2004).
23. Wang, W.U., Chen, C., Lin, K.H., Fang, Y. & Lieber, C.M. Label-free detection of small-molecule–protein interactions by using nanowire nanosensors. *Proc. Natl. Acad. Sci. USA* **102**, 3208–3212 (2005).
24. Armbruster, D.A. Prostate-specific antigen: biochemistry, analytical methods and clinical application. *Clin. Chem.* **39**, 181–195 (1993).
25. Pomerantz, M., Segmuller, A., Netzer, L. & Sagiv, J. Coverage of Si substrates by self-assembling monolayers and multilayers as measured by IR, wettability and x-ray diffraction. *Thin Solid Films* **132**, 153–162 (1985).
26. Heiney, P.A., Gruneberg, K., Fang, J.Y., Dulcey, C. & Shashidhar, R. Structure and growth of chromophore-functionalized (3-aminopropyl)triethoxysilane self-assembled on silicon. *Langmuir* **16**, 2651–2657 (2000).
27. Sze, S.M. *Physics of Semicondutor Devices* (John Wiley & Sons, New York, 1981).
28. Lilja, H. *et al.* Prostate-specific antigen in serum occurs predominantly in complex with α_1-antichymotrypsin. *Clin. Chem.* **37**, 1618–1625 (1991).
29. Stenman, U.H. *et al.* A complex between prostate-specific antigen and α_1-antichymotrypsin is the major form of prostate-specific antigen in serum of patients with prostatic cancer: assay of the complex improves clinical sensitivity for cancer. *Cancer Res.* **51**, 222–226 (1991).
30. Martinez, M. *et al.* The proportion of prostate-specific antigen (PSA) complexed to α_1-antichymotrypsin improves the discrimination between prostate cancer and benign prostatic hyperplasia in men with a total PSA of 10 to 30 μg/L. *Clin. Chem.* **48**, 1251–1256 (2002).
31. Moyzis, R.K. *et al.* A highly conserved repetitive DNA-sequence, (TTAGGG)N, present at the telomeres of human-chromosomes. *Proc. Natl. Acad. Sci. USA* **85**, 6622–6626 (1988).
32. Morin, G.B. The human telomere terminal transferase enzyme is a ribonucleoprotein that synthesizes TTAGGG repeats. *Cell* **59**, 521–529 (1989).
33. O'Reilly, M., Teichmann, S.A. & Rhodes, D. Telomerases. *Curr. Opin. Struct. Biol.* **9**, 56–65 (1999).
34. Rhyu, M.S. Telomeres, telomerase and immortality. *J. Natl. Cancer Inst.* **87**, 884–894 (1995).
35. Shay, J.W. & Bacchetti, S. A survey of telomerase activity in human cancer. *Eur. J. Cancer* **33**, 787–791 (1997).
36. Kim, N.W. *et al.* Specifc association of human telomerase activity with immortal cells and cancer. *Science* **266**, 2011–2015 (1994).
37. Nugent, C.I. & Lundblad, V. The telomerase reverse transcriptase: components and regulation. *Genes Dev.* **12**, 1073–1085 (1998).
38. Shippen-Lentz, D. & Blackburn, E.H. Functional evidence for an RNA template in telomerase. *Science* **247**, 546–552 (1990).
39. Hirose, M. *et al.* A rapid, useful and quantitative method to measure telomerase activity by hybridization protection assay connected with a telomeric repeat amplification protocol. *J. Cancer Res. Clin. Oncol.* **123**, 337–344 (1997).
40. Gelmini, S. *et al.* Rapid, quantitative nonisotopic assay for telomerase activity in human tumors. *Clin. Chem.* **44**, 2133–2138 (1998).
41. Uehara, H., Nardone, G., Nazarenko, I. & Hohman, R.J. Detection of telomerase activity utilizing energy transfer primers: comparison with gel- and ELISA-based detection. *Biotechniques* **26**, 552–558 (1999).
42. Szatmari, I., Tokes, S., Dunn, C.B., Bardos, T.J. & Aradi, J. Modified telomeric repeat amplification protocol: a quantitative radioactive assay for telomerase without using electrophoresis. *Anal. Biochem.* **282**, 80–88 (2000).
43. Wege, H., Chui, M.S., Le, H.T., Tran, J.M. & Zern, M.A. SYBR Green real time telomeric repeat amplification protocol for the rapid quantification of telomerase activity. *Nucleic Acids Res.* **31** (No. 2 e3), 1–7 (2003).
44. Mitsuya, H., Yarchoan, R. & Broder, S. Molecular targets for AIDS therapy. *Science* **249**, 1533–1544 (1990).
45. Miyashita, M., Shimada, T., Miyagawa, H. & Akamatsu, M. Surface plasmon resonance-based immunoassay for 17 beta-estradiol and its application to the measurement of estrogen receptor-binding activity. *Anal. Bioanal. Chem.* **381**, 667–673 (2005).
46. Haes, A.J., Hall, W.P., Chang, L., Klein, W.L. & Van Duyne, R.P. A localized surface plasmon resonance biosensor: first steps toward an assay for Alzheimer's disease. *Nano Lett.* **4**, 1029–1034 (2004).
47. Cui, Y., Zhong, Z., Wang, D., Wang, W.U. & Lieber, C.M. High performance silicon nanowire field effect transistors. *Nano Lett.* **3**, 149–152 (2003).
48. Zheng, G., Lu, W., Jin, S. & Lieber, C.M. Synthesis and fabrication of high-performance n-type silicon nanowire transistors. *Adv. Mater.* **16**, 1890–1893 (2004).
49. Wong, P.K., Chen, C.-Y., Wang, T.-H. & Ho, C.-M. Electrokinetic bioprocessor for concentrating cells and molecules. *Anal. Chem.* **76**, 6908–6914 (2004).